



Research Article

Performance comparison and investigation of two different renewable energy fueled multigeneration systems

Parisa HEIDARNEJAD¹, Alireza NOORPOOR^{1,*}

¹School of Environment, College of Engineering, University of Tehran, Tehran, Iran

ARTICLE INFO

Article history

Received: 22 May 2019

Accepted: 21 August 2019

Key words:

Biomass; Environmental assessment; Exergoeconomic; Exergy; Multigeneration; Solar

ABSTRACT

In this study, the comprehensive thermodynamic, exergoeconomic and environmental performance of two multigeneration systems fuelled by biomass and solar energy is surveyed. The multigeneration system A utilizes municipal solid waste and solar energy to produce power, heating, cooling, fresh water, and hydrogen which is considered to be located in the north of Iran with a moderate climate. Whereas, the multigeneration system B consumes bagasse and solar energy to supply power, heating, cooling, liquefied natural gas, and freshwater which is assumed to be located in the south of Iran with a hot climate. The results of the study show that system B provides better performance from a thermodynamic viewpoint with energy and exergy efficiencies of 82.45% and 15.75%. Moreover, according to the outputs of exergoeconomic modelling, system B presents better performance because of lower capital costs. Finally, environmental profit is attained by accomplishing system B because of avoiding 1.14 million tons of NO_x and 0.31 million tons of CO₂ depletion to the atmosphere per year. In the end, through conducting a parametric study, the effect of key parameters on the thermodynamic, economic, and environmental performances of two systems is discussed.

Cite this article as: Heidarnajad P, Noorpoor A. Performance comparison and investigation of two different renewable energy fueled multigeneration systems. J Thermal Eng 2021;7(5):1039-1055.

INTRODUCTION

In recent years, researchers have focused on renewable energy fuelled integrated energy systems as a promoted solution to enhance the efficiency of energy systems, lower fossil fuel depletion and lower environmental effects. Multi-generation systems are presented as energy systems

which have the ability to supply different commodities simultaneously. Due to the complexity of the multi-generation systems, the arrangement, demand type, climate zone, and the available energy sources, the design of these systems necessitates detailed examination. Therefore, applying a universal model to extract the design of the

*Corresponding author.

*E-mail address: noorpoor@ut.ac.ir

This paper was recommended for publication in revised form by Regional Editor Mustafa Kılıç



system is fundamental. Several studies have focused on energy, exergy, economic and environmental analyses of multi-generation systems with renewable energies as input. For example, Boyaghchi and Heidarnajad [1] proposed the model of a CCHP (Combined Cooling, Heating and Power) system with the purpose of thermodynamic and thermoeconomic and determined the optimum design of the system by employing GA (Genetic Algorithm). Findings showed that exergy efficiency and product cost rate increases by 27% and 17% in summer cases and 13% and 4% in winter cases. Economic and environmental analyses of a biomass fed multi-generation system were carried out by Jana and De [2]. Results presented that up to 20% reduction in energy consumption and 25kt/y avoidance of CO₂ discharge is achievable. Caliskan [3] performed a comparative analysis of renewable and natural gas as energy sources for a building including thermodynamic, economic and environmental viewpoints. It was presented that the system with solar energy is the most favourable. Noorpoor et al. [4] suggested a thermodynamic model for a multi-generation system based on biomass and solar energy with the purpose of generating electricity, water, cooling, and heating. The role of applying optimisation methods in trigeneration systems was represented by Al Moussawi et al. [5] in which the categories of optimisation and decision making methods were investigated. In a study, Bellos and Tzivanidis [6] proposed a solar fuelled trigeneration system operating with different fluids. They presented that Toluene yields the best performance. Khanmohammadi et al. [7] developed a comprehensive model for a solar-based integrated system. In a study, Di Somma et al. [8] introduced the distributed energy systems as a promising alternative for sustainable development. They applied the exergy principles as a complementary tool to economic assessment to design a sustainable energy supply. The innovation of this research is specifying the best structure of the distributed energy system regarding minimising total annual cost and maximising the exergy efficiency. The results showed that the total annual cost is reduced by 21% while the exergy input to the system is reduced by 36% in the optimal case in comparison to the base case. Calise et al. [9] suggested a novel multi-generation system for an island in Italy to provide electric power, freshwater, cooling, and heating consuming solar and geothermal sources. Ganjehsarabi et al. [10] conducted the thermodynamic modelling of a solar-assisted integrated system in terms of energy and exergy analyses. They pointed out that by integrating the solar organic Rankine cycle, its exergy efficiency improves about 5%. In comparative research, Sahoo et al. [11] studied the advantages of a solar and biomass-fuelled multi-generation system. Results indicate that the studied system has the potential to produce energy 78.12% higher than the conventional system. Bellos and Tzivanidis [12] performed the optimisation of a solar-based CCHP system. In this study, thermodynamic

efficiencies and savings cash flow were nominated as the objective functions. The thermodynamic modelling of an integrated energy system applying waste energy of biomass gasification was evaluated by Boyaghchi et al. [13]. In the mentioned research, two decision-makers were introduced to define the optimum scheme. Thermodynamic, thermoeconomic and multi-criteria optimisation of biomass and solar fuelled multi-generation system was conducted by Ghasemi et al. [14]. Multi-objective optimisation caused to extract the Pareto front. In another work, the prediction of the performance of a novel polygeneration system based on biomass gasification was performed by Khanmohammadi and Atashkari [15]. In this study, the findings of exergy modelling presented that the gasifier and combustion chamber contributes 84% of the total irreversibilities. Moreover, the multi-criteria optimisation using GA has been applied in this research to find the optimal states of the studied configuration considering two conflicting objective functions such as exergy efficiency and total cost rate. Yilmaz [16] performed the sensitive analysis of a solar-based multi-generation system considering the thermodynamic aspect. It resulted that the mentioned system produces 19MW electricity with energy and exergy efficiencies of 79% and 48%, respectively. Wang et al. [17] developed a detailed optimisation model of an integrated energy system regarding economics, autonomy and carbon emissions. In a different study including energy and exergy analysis of fuel cell-based integrated energy system, Nalbant et al. [18] presented a novel approach of assessing the integrated energy system with renewable sources. The results demonstrated that the stoichiometric ratio of the anode is the most influential parameter which affect the exergetic efficiency up to 37.4%. Ganjehsarabi [19] investigated the thermodynamic and thermoeconomic performances of a geothermal based integrated energy system by trying different mixed refrigerants as the working fluid of the cycle.

Since the type of demand, environmental conditions like the type of biomass and the intensity of solar radiation and environment temperature are associated to the climate zone; it is one of the parameters which affect the efficiency of multi-generation systems. Some studies have surveyed the effect of the climate zone on the productivity of the multi-generation systems. Mateus and Oliveira [20] evaluated the performance of a solar fuelled integrated energy system for three different climate zone in Germany, Portugal, and Italy as well as for three types of building such as residential, hotel and office. comprehensive assessment of a BCCHP (Building Combined Cooling Heating and Power) system for five climate zones of China were investigated by Jiang-Jiang et al. [21]. Sigarchian et al. [22] assessed the performance of three multi-generation systems from thermodynamic, economic and environmental viewpoints. Results presented that in cold climate zones, the multi-generation system yields the reduction

of CO₂ emission to about 27% while this value is 41% for hot climate zones. In a comparative study, the impact of the system configuration on the thermodynamic and thermoeconomic performances of two trigeneration system based on industrial waste heat was assessed by Heidarnejad et al. [23]. In the mentioned study, the energy and exergy efficiencies and product cost rate of both systems were studied and discussed. In two complementary studies, Doseva and Chakyrova [24, 25] presented the thermodynamic and thermoeconomic analyses of a biogas based cogeneration plant which is located in Bulgaria. The energetic and exergetic efficiencies of the plant calculated to be 53.3% and 34.6%. Thermoeconomic modelling was performed based on SPECO (specific exergy cost) method which resulted to achieve a cost for produced electric power by system of about 0.19 €/kWh.

In order to specify the effect of geographical region on thermodynamic, economic and environmental performances of the integrated energy systems, two multi-generation systems with different sources and productions are regarded and investigated for north and south regions of Iran. This case has not been taken into account by previous researchers which can be addressed by modelling and comparing the performance of two multigeneration systems driven by biomass and solar energy in two cities (Sari and Ahvaz) of Iran. System A is considered to be located in Sari city with the problem of surplus MSW (Municipal Solid Waste). System B is assumed to be located in Ahvaz city with rich resources of natural gas which is proposed to be converted to the LNG. In the present work, exergoeconomic analysis and environmental evaluation of both systems as well as energetic and exergetic modelling are performed. The comparative study is applied based on comprehensive analyses in order to evaluate the feasibility of multi-generation systems regarding the available sources, type of demands and geographical region.

THEORY

The energetic, exergetic, economic and environmental modelling of two proposed multi-generation systems which is explained below is performed by developing code in EES (Engineering Equation Software) software [26] on the basic of energy, exergy and exergoeconomic balances applied for each component of both systems. Finally, the environmental assessment of system A and system B is carried out regarding emission factors related to renewable energy sources and fossil fuels.

The layouts of multi-generation system A and multi-generation system B are illustrated in Figure 1. As it is clear in Figure 1, system A includes PTC (Parabolic Trough Solar Collectors), MSW combustion chamber, Rankine cycle, heat exchanger, DEAC (Double Effect Absorption Chiller), MED (Multi Effect Desalination) and PEM (Proton Exchange Membrane) electrolyser. Solar

energy and energy of MSW combustion have utilised the system A. The oil circulating in the tube of the collector is Therminol VP-1 and absorbs the heat of solar energy. On the other hand, MSW is combusted as an auxiliary fuel to eliminate the fluctuations of solar energy in order to have a constant supply. The steam of the Rankine cycle absorbs the provided heat and enters the turbine to produce electricity through an electric generator. A share of electricity is utilised by PEM electrolyser to separate water into hydrogen and oxygen. The output stream of the turbine is hot enough to make heating and cooling effects in the heat exchanger and DEAC, respectively. Hot gasses leaving the combustor have sufficient energy to drive a MED and extract the freshwater from seawater during a four-stage evaporation and condensation process.

As it is obvious in Figure 1, system B is identical to system A except for the bagasse combustion chamber and LNG (Liquefied Natural Gas) subsystem. In this system, bagasse as a valuable agricultural waste is combusted in the combustor as a complementary resource. The fraction of electricity generated by the electric generator is consumed by the compressor of the LNG subsystem in order to raise the pressure of natural gas to the desired pressure. Then the gas is passed along a throttling valve and converted to liquid natural gas.

Thermodynamic and exergoeconomic analyses and environmental investigation of two multi-generation systems are accomplished through the below assumptions:

- (a) The subsystems function at steady-state and potential and kinetic energies and exergies are negligible.
- (b) The pressure and heat losses in the pipes and thermal equipments excluding MED are not taken into account.
- (c) The dead state condition is assumed to have a temperature of 298 K and a pressure of 100 kPa.
- (d) The natural gas and air are assumed to be ideal gasses.
- (e) Isentropic efficiencies of turbines and pumps are presumed to be 80% and 70%.
- (f) The seawater salinity is considered to be 40 g/kg.
- (g) The desalination subsystem has four effects.
- (h) The sun temperature is considered $T_s = 6000$ K.
- (i) Working fluid of double effect absorption chiller is the solution of LiBr-H₂O.
- (j) Higher heating values of MSW and bagasse are approximately equal to chemical exergy [27], and efficiencies of both combustors are 80%.
- (k) The operating temperature in the evaporator of DEAC is 10°C.
- (l) Average monthly solar radiation on the horizontal surface and average air temperature for Sari and Ahvaz cities are considered according to the amounts reported in [28] (See Figures 2 and 3).

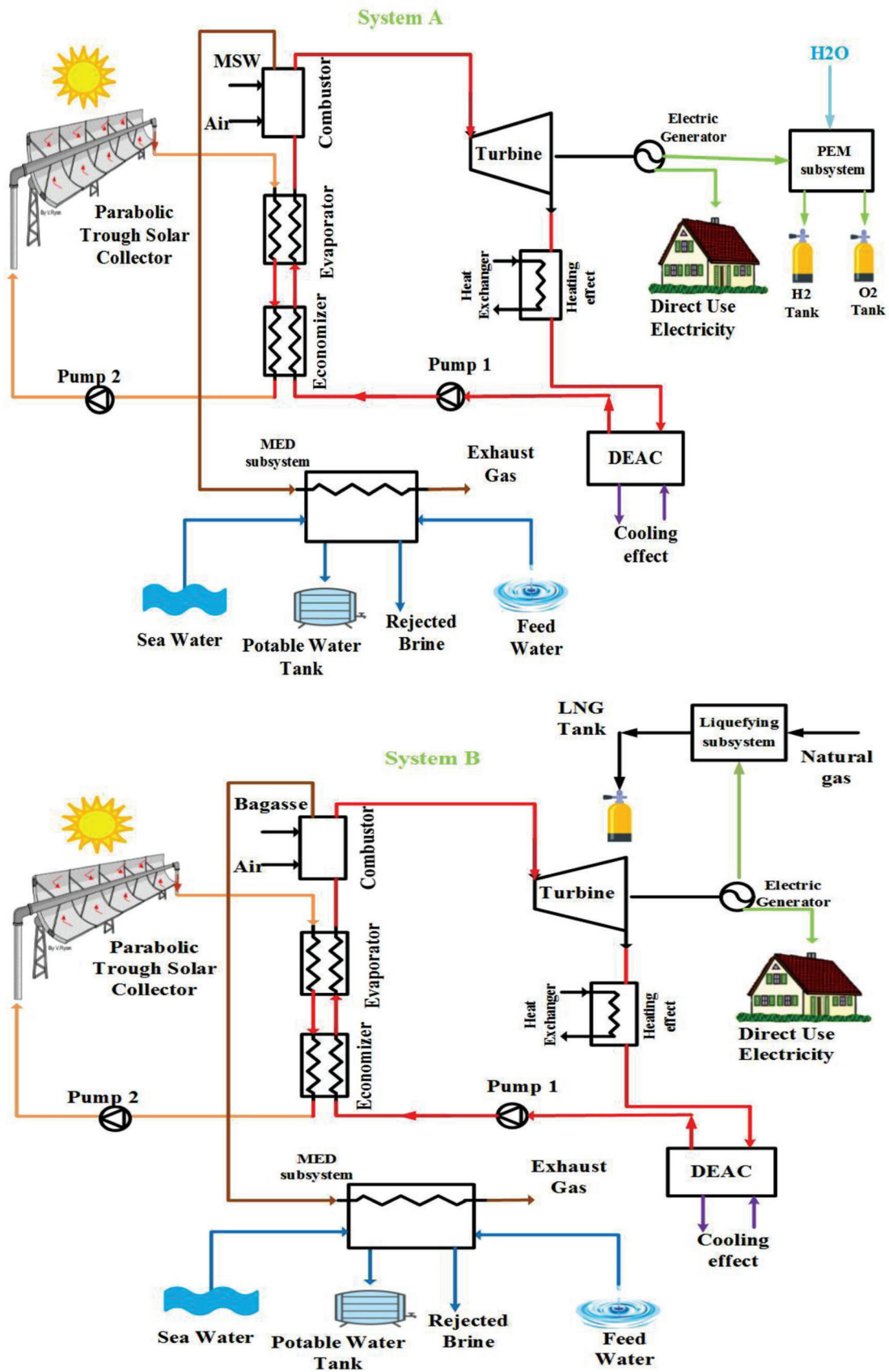


Figure 1. The schematics of multi-generation system A and multi-generation system B.

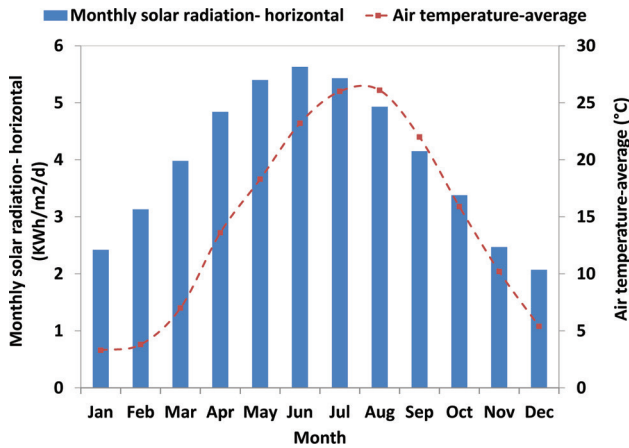


Figure 2. Average monthly solar radiation on the horizontal surface and average air temperature for Sari city (36.5659° N, 53.0586° E).

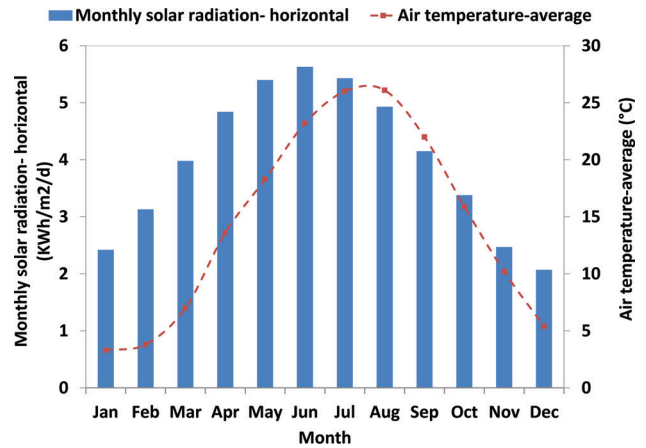


Figure 3. Average monthly solar radiation on the horizontal surface and average air temperature for Ahvaz city (31.3183° N, 48.6706° E).

Energetic and Exergetic Modeling

Energetic and exergetic modelling is performed based on forming energy and exergy balances for each component of the two proposed multi-generation systems in a steady-state process as below:

$$\dot{Q} + \sum \dot{m}_in \left(h_in + \frac{1}{2} V_in^2 + gz_in \right) = \sum \dot{m}_out \left(h_out + \frac{1}{2} V_out^2 + gz_out \right) + \dot{W} \quad (1)$$

$$\left(1 - \frac{T_0}{T_i} \right) \dot{Q}_i + \sum \dot{m}_in ex_in = \sum \dot{m}_out ex_out + \dot{W} + \dot{E}x_D \quad (2)$$

where \dot{Q} and \dot{W} are related to heat and work rate passing through the boundaries, \dot{m} represents the mass flow rate, h and s corresponds to specific enthalpy and entropy, $\dot{E}x_D$ and T_i indicate the exergy destruction rate and the temperature in which heat transfer occurs.

Specific exergy of a mass flow comprises of physical and chemical exergy parts:

$$ex = ex^{ph} + ex^{ch} \quad (3)$$

$$ex^{ph} = (h - h_0) - T_0 (s - s_0) \quad (4)$$

$$ex^{ch} = \left[\sum_{i=1}^n x_i ex_i^{ch} + RT_0 \sum_{i=1}^n x_i \ln x_i \right] \quad (5)$$

According to the above equations, energy and exergy equations for subsystems of the polygeneration systems are

formed and given through Tables 1 and 2, respectively in Appendix A.

Exergoeconomic Modeling

Exergoeconomic modelling is a consolidated tool of exergy and economic methods which has the capability in determining the cost flows and product cost rate in the integrated energy systems considering the role of inefficiencies of the components. In this section, exergoeconomic balances are formulated for each subsystem of the two multi-generation systems as below and are presented in Appendix B, Table 3 in order to evaluate the exergoeconomic performance of the studied systems for better comparison [29, 30]:

$$\sum_k (c_{out} \dot{E}x_{out})_k + c_{w,k} \dot{W}_k = c_{q,k} \dot{E}x_{q,k} + \sum_k (c_{in} \dot{E}x_{in})_k + \dot{Z}_k \quad (6)$$

$$C_i = c_i Ex_i \quad (7)$$

$$\dot{Z}_k = \dot{Z}_k^{CI} + \dot{Z}_k^{OM} = \frac{CRF \times \delta \times PEC_k}{N \times 3600} \quad (8)$$

$$CRF = \frac{i(1+i)^n}{(1+i)^n - 1} \quad (9)$$

In which \dot{Z}_k is donated for investment cost rate of the kth component which is the summation of capital investment and operating and maintenance costs. c_w and c_q account for

cost per exergy of work and heat. The maintenance factor (δ) is assumed to be 1.06 and the annual operation hours of the system (N) is usually considered to be 7446 h/year. PEC_k of all subsystems of two multi-generation systems are listed in Appendix B, Table 3. i and n account for the interest rate and lifetime of the system which is considered to be 10% and 20 years.

Environmental Impact Assessment

The assessment of any type of emission from any combustion process is performed applying its relevant emission factor. Because of the high concentration of CO_2 and NO_x emissions among other greenhouse gas emissions and pollutants, the amount of CO_2/NO_x emitted along with any useful output of the system is obtained through the following model:

$$m_{CO_2,NO_x} = \phi_{CO_2,NO_x}^P \cdot P \quad (10)$$

Where P in general can be used for any type of output like electricity, cooling or heating in kWh and ϕ_{CO_2,NO_x}^P is the emission factor for producing any kind of energy output and is defined in kg/kWh as the amount of CO_2/NO_x emitted per unit of energy output. In the other hand, the amount of CO_2/NO_x emission from a process depends on the type of fuel combusted specifically carbon content, combustion condition, and heating value as well as the efficiency of the energy conversion device. Therefore the equation (10) can be rewritten by assuming a different factor ϕ_{CO_2,NO_x}^F presenting the amount of CO_2/NO_x emitted per unit of energy input to the device. Regarding the ratio of energy output to energy input as related efficiency, the equation (10) can be converted to a function of emission factor of energy input, the amount of energy input F and the efficiency of the device simultaneously as below:

$$m_{CO_2,NO_x} = \phi_{CO_2,NO_x}^P \cdot P = \phi_{CO_2,NO_x}^F \cdot \frac{P}{\eta} = \phi_{CO_2,NO_x}^F \cdot F \quad (11)$$

Where η is the efficiency related to the generation of the specific amount of P from the energy input of F .

Emission reduction (ER) brought by the renewable energy based multi-generation systems can be introduced by ER indicator through the below relation. ER indicator highlights the privilege of integrating renewable energy sources with multi-generation systems to multi-generation systems using fossil fuels. The ER indicator is calculated as follows:

$$ER_{CO_2,NO_x} = \frac{(m_{CO_2,NO_x})^{RN} - (m_{CO_2,NO_x})^{FF}}{(m_{CO_2,NO_x})^{FF}} \quad (12)$$

In which, $(m_{CO_2,NO_x})^{RN}$ and $(m_{CO_2,NO_x})^{FF}$ are referred to the amount of CO_2/NO_x emission related to the multi-generation system fuelled by renewable energy and fossil fuel, respectively.

RESULTS AND DISCUSSION

In this section, results of energy, exergy and exergoeconomic modelling of two studied systems are presented and discussed. The mathematical model extracted from the mentioned equations is solved by means of EES software. System1 is considered to be located in the north of Iran with a moderate climate and have sufficient amounts of MSW while the second system is considered to be located in the south of Iran with a hot climate and benefits from sufficient amounts of bagasse as a by-product of sugarcane. The findings of the modelling of systems illustrated in Figure 1 are shown in Table 4 and Figures 4–6. As it is presented in Table 4, the amounts of power, cooling, and heating energy are lower for system A due to the lower mass flow rate of working fluid in the cycle which results in lower energy and exergy performances. Since the average of solar radiation on a horizontal surface for Ahvaz is higher than Sari, the share of solar energy in total energy input to system B (solar fraction) is calculated to be 86% which means consuming less biomass while this value is 44% for the system A.

Results of exergoeconomic analysis such as investment cost rates are achieved based on the results of exergoeconomic modelling and demonstrated by Figure 4. It is concluded that system B is more affordable regarding the lower investment cost rate. As it is clear, the investment cost rate of the turbine is higher for system A while the investment cost rate of biomass combustor is lower. The higher investment cost rate of biomass combustor in system A is achieved due to requiring the larger capacity of MSW combustor to cover the lower LHV and lower solar fraction.

According to emission factors reported by [33–35] and heat values listed in Table 4 for natural gas, MSW and bagasse combustion, the amount of CO_2 and NO_x emission for both systems in two modes are calculated and demonstrated in Figures 5 and 6.

Considering the multi-generation system A in two modes, the results of the environmental assessment are obtained; mode1 (Sys A-FF): the system using natural gas as an energy source while in mode 2 (Sys A-MSW): the system benefiting MSW combustion and solar energy to yield the same outputs. According to the results, system A requires 279.84 MW of primary energy to provide the products which are supplied in mode 1 by natural gas combustion in a boiler with an average efficiency of 80%. Assuming the emission factors for natural gas $\phi_{CO_2}^{NG} = 183kgCO_2 / MWh$ [36] and $\phi_{NO_x}^{NG} = 0.15kgNO_x / MWh$ [33], the amount of CO_2 and NO_x discharged by system B in mode 1 is calculated (Figures 5 and 6). In mode 2, system1 is fed by solar

Table 1. Thermodynamic performances of system A and system B

Performance parameter	System A	System B	Performance parameter	System A	System B
Total energy input (MW)	253.28	230	Generated hydrogen (kg/h)	587.60	-
Energy input by solar energy (MW)	112.40	198.69	Exergy of generated hydrogen (kW)	25.48	-
Total exergy input (MW)	344.16	231.27	Generated LNG (kg/h)	-	3,279
Exergy input by solar energy (MW)	104.96	185.54	Exergy of generated LNG (MW)	-	38.23
Exergy input by MSW combustion (MW)	239.20	-	Total exergy destruction rate (MW)	311.59	212.35
Exergy input by bagasse combustion (MW)	-	45.71	MSW feed (kg/s)	82.45	-
Generated electricity (MW)	30.33	31.28	Bagasse feed (kg/s)	-	5.31
Generated heating power (MW)	20.76	21.40	Solar fraction (%)	44	86
Exergy of heating power (MW)	3.41	3.52	LHV of bagasse* (kJ/kg)	-	6,903
Generated cooling power (MW)	113.10	137.17	LHV of MSW** (kJ/kg)	2,716	-
Exergy of cooling power (MW)	3.42	3.53	LHV of natural gas (kJ/kg)	45,543	-
Generated fresh water (m ³ /h)	187.78	12.09	Energy efficiency (%)	85.27	82.45
Exergy of generated fresh water (MW)	5.10	0.33	Exergy efficiency (%)	11.4	15.75

* LHV of bagasse is estimated through Von Pritzelwitz formula provided by [31] and bagasse characterisation for Ahvaz.

** The prediction of LHV is based on the formulation provided by Dulong [32] and waste characterisation for Sari.

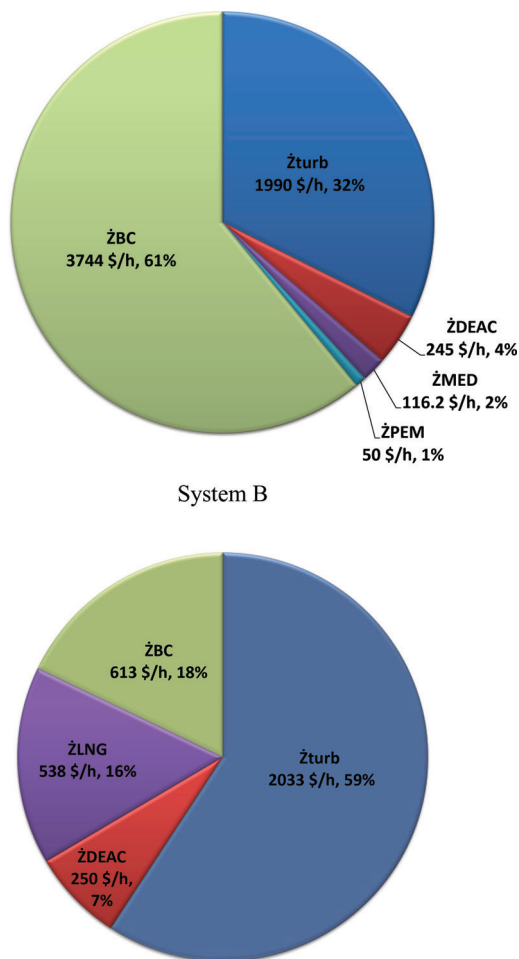


Figure 4. Exergoeconomic performance of system A and system B.

energy with zero-emission and the heat of MSW combustion. Considering the emission factors for MSW $\phi_{NO_x}^{MSV} = 313kgCO_2/MWh$ [36] and $\phi_{NO_x}^{MSV} = 0.66kgNO_x/MWh$ [37], the amount of CO_2 and NO_x emitted by system A in mode 2 is calculated and reported in Figures 5 and 6.

Multi-generation system B is investigated in two modes; mode1 (Sys B-FF): the system using natural gas as an energy source while in mode 2 (Sys B-Bag): the system utilising bagasse combustion and solar energy to provide the same products. System B requires 228.32 MW of primary energy to provide the products and is fed in mode 1 by natural gas combustion in a boiler with an average efficiency of 80%. Assuming the emission factors for natural gas, the amount of emission by system B in mode 1 is calculated. In mode 2, system B is fed by solar energy and the heat of bagasse combustion. Assuming the emission factors for bagasse $\phi_{NO_x}^{NG} = 329kgNO_x/MWh$ [36] and $\phi_{NO_x}^{MSV} = 66kgNO_x/MWh$ [34], the amount of emission by system B in mode 2 is calculated and reported in Figures 5 and 6.

Obviously, the CO_2 and NO_x emission of multi-generation system A is higher than of multi-generation system B. This is observed because; the heat value of bagasse is more than MSW (see Table 4) which leads to consume more biomass fuel in system A in comparison to system B.

Focusing on the ER indicators of both systems, it is concluded that by applying renewable sources in system A in the northern region of Iran, about 1.3 million tons of NO_x are avoided annually to discharge to the atmosphere ($ER_{NO_x} = 90\%$). Besides, it is a sustainable solution for solid waste management in that area.

On the other hand, system B with renewable energy and sources presents significant environmental benefits in

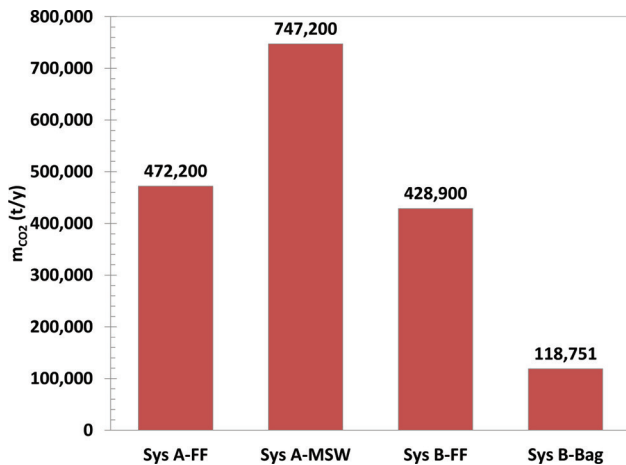


Figure 5. Amount of CO_2 emissions for system A and system B.

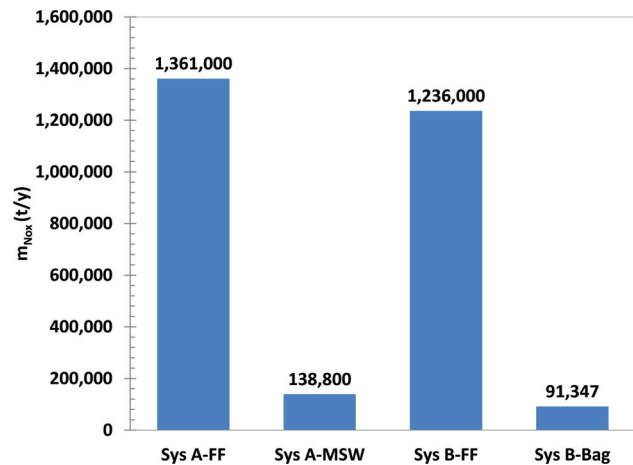


Figure 6. Amount of NO_x emissions for system A and system B.

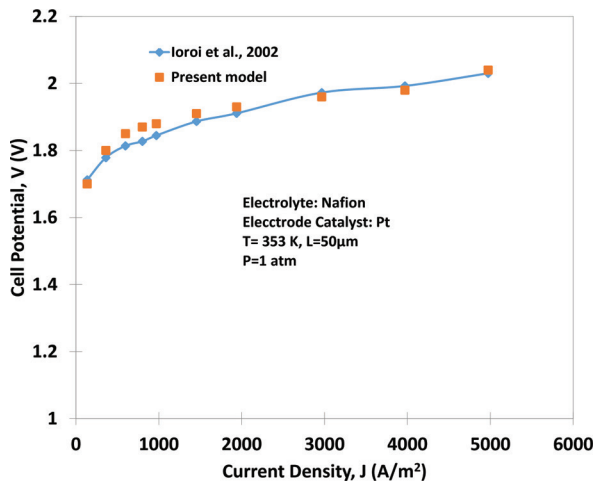


Figure 7. Validation of PEM model.

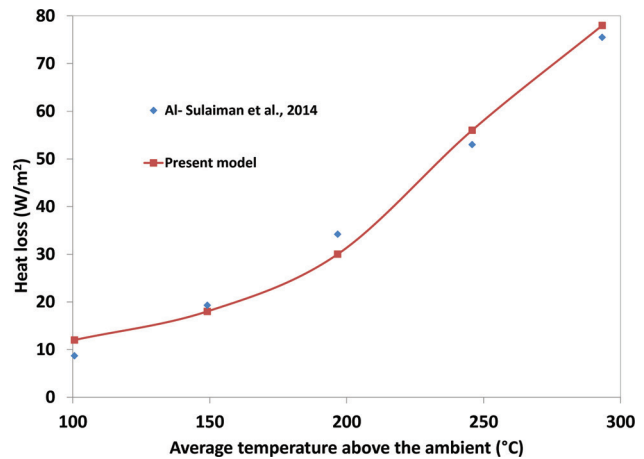


Figure 8. Validation of PTC model.

the southern region of Iran so which leads to the avoidance of about 0.3 million tons of CO_2 emissions to the atmosphere ($ER_{CO_2} = 72\%$). Moreover, system B prevents the emission of NO_x to about 1.14 million tons annually with $ER_{NO_x} = 93\%$. Furthermore, consuming the unemployed bagasse in that area efficiently is the positive side effect of applying biomass and solar energy as the fuel of system B.

These achievements point out the superiority of renewable energy based multi-generation system to conventional ones.

Validation of PEM and PTC

For proving the reliability of the results, the model of the main components should validate with data provided in the literature review. The PEM model is compared with experimental data of [38]. The results are provided in

Figure 7. Moreover, the PTC model has been validated with the results of [39] and are shown in Figure 8. According to Figures 7 and 8 there is a good agreement between the present model of PEM and PTC and mentioned studies.

Parametric Study

In this segment, the results gained from the effect of two key parameters on the thermodynamic, economic and environmental performances of system A and system B are discussed and compared. In this manner, local time and LHV are selected as understudy parameters. On the other hand, the impact of these parameters are surveyed on the energy and exergy efficiencies, investment cost rate and the amount of NO_x and CO_2 emissions of system and system B through Figures 9–11.

The effect of the lower heat value of bagasse and MSW on energy and exergy efficiencies is plotted in Figure 9(a).

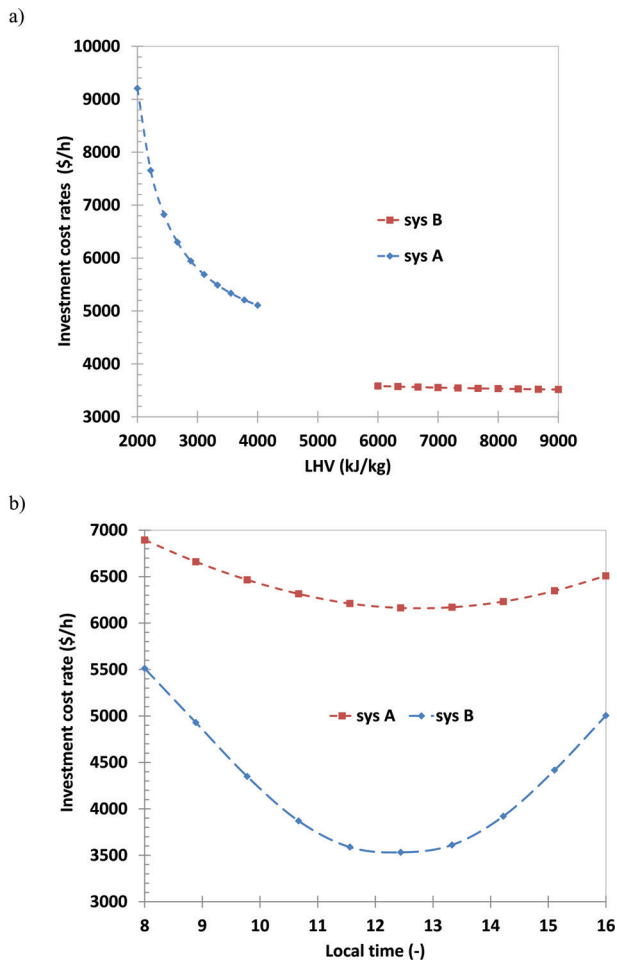


Figure 9. a) The effect of LHV on energy and exergy efficiencies of system A and system B, b) the variation of energy and exergy efficiencies of system A and system B during a day.

As observed with the rise of LHV, the energy and exergy efficiencies of both systems would increase negligibly because lower LHV means higher mass flow rate of biomass required maintaining the production constant and as a result, the energy and exergy fed to the system A and system B by biomass energy are almost unchanged. The variation of energy and exergy efficiencies of system A and system B in a day is shown in Figure 9(b). It is seen that the energy efficiencies of both systems have the minimum values in the midday, 85.21% for system A and 85.33% for system B. On the other hand, in the midday, maximum values of exergy efficiencies occur which means the best exergetic performance for both systems, 11.44% for system A and 15.64% for system B.

In Figure 10(a), the effect of the lower heat value of bagasse and MSW on investment cost rates is displayed. Accordingly as shown in this figure, an increase in the LHV has brought about a decrease in the investment cost

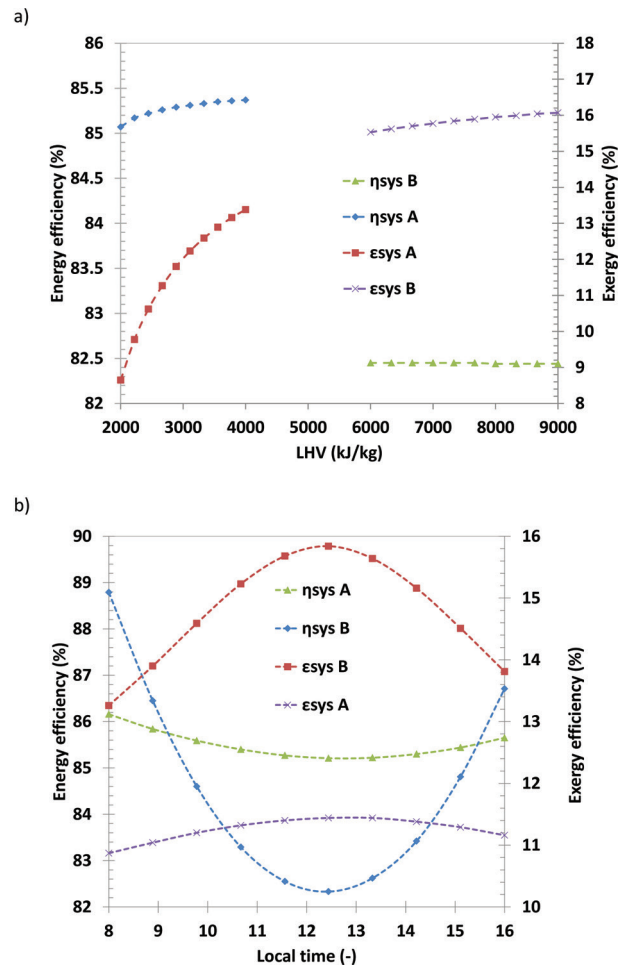


Figure 10. a) The effect of LHV on investment cost rates of system A and system B, b) the variation of investment cost rates of system A and system B during a day.

rates of system A and system B as much as 45% and 2%, respectively. This phenomenon occurs because consuming biomass with higher LHV causes a lower biomass mass flow rate and as a result lower investment cost rate of biomass combustor. Additionally, the variation of investment cost rates of system A and system B during a day is graphed in Figure 10(b). As seen, due to an increase in the energy input to the system by solar energy in the midday, the investment cost rates of solar collectors and biomass combustor reach their minimum values, therefore the overall investment cost rates of system A and system B decreases.

At the end of parametric analysis, the examination of the effect of LHV and local time on the amount of CO_2 and NO_x emission for system1 and system B is addressed in Figures 11(a) and 9(b), respectively. It is observed that consuming the biomass with higher LHV results in a reduction of NO_x emission (about 62% for system1 and about 40%

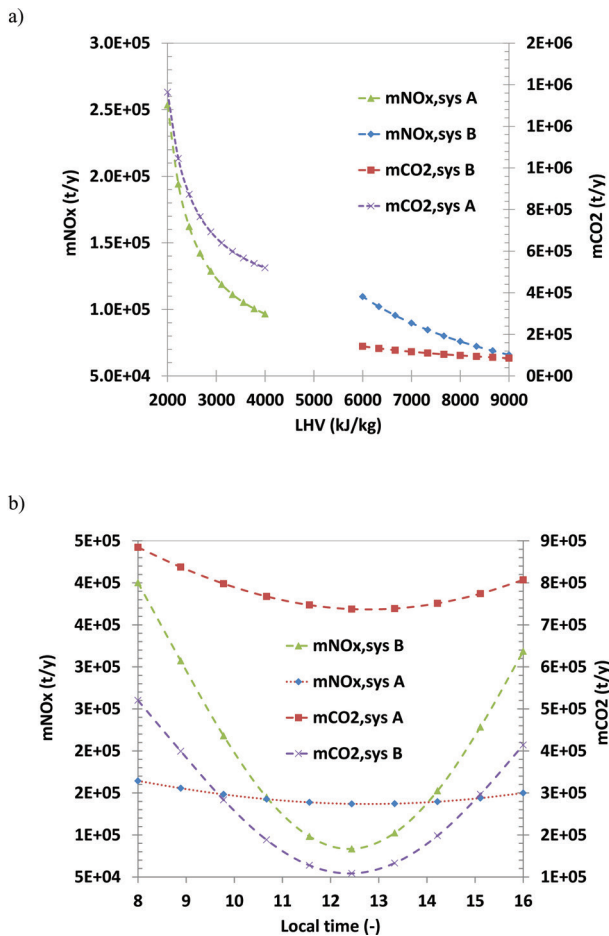


Figure 11. a) The effect of LHV on the amount of CO₂ and NO_x emission for system1 and system B, b) the variation of the amount of CO₂ and NO_x emission for system1 and system B during a day.

for system B) and also the rate of CO₂ emission (about 62% for system1 and about 40% for system B). As illustrated in Figure 11(b), the amount of NO_x emission for system1 and system B reaches minimum values in the midday (138,817 t/y for system1 and 91,347 t/y for system B). The highest amount of solar radiation takes place in the midday which results in a decrement of required biomass as a backup fuel. Therefore the amount of CO₂ and NO_x emission for both systems drops.

CONCLUSION

In this study, two solar and biomass-based multi-generation systems are proposed for the north and south of Iran and analysed thermodynamically, economically and environmentally. System A is fed by MSW and solar energy and system B utilizes bagasse and solar energy. Both systems are similar in productions except for hydrogen in the

first one and LNG in the second one. Results demonstrate that system B performs more efficiently from a technical viewpoint with energy and exergy efficiencies of 82.45% and 15.75%. This occurs because system A compensates for the shortcoming of solar energy by combusting more biomass with a lower heat value in comparison to system B. From the viewpoints of exergoeconomic, system B is more desired, because requiring more biomass energy means the larger capacity of biomass combustor which leads to higher investment cost for system A. Further, the assessment of environmental effects reveals that system B with avoidance of 1.14 million tons of NO_x and 0.3 million tons of CO₂ emissions is more beneficial than the same system driven by natural gas. Finally, a comprehensive parametric study is conducted in order to investigate the role of key parameters like LHV of biomass and local time in the thermodynamic, economic and environmental performances of system1 and system B. From the results, it is concluded that the regions with higher intensity of solar radiation and heating value of biomass as a backup fuel are favourable for establishing multigeneration systems.

Since multi-generation systems are complex networks consisting of multiple sources, multiple commodities and diverse configurations, the comparative and comprehensive study assist to extract a strategy of designing these systems for different locations, available sources and demands in a country considering technical, economic and environmental limits with the purpose of maximum profitability.

NOMENCLATURE

A_a	Aperture area (m ²)
A_r	Receiver area (m ²)
C_p	Specific heat capacity
c	Cost per exergy unit (\$/kW)
\dot{C}	Cost rate (\$/s)
D_L	Membrane thickness
E_{act}	Activation energy
ex	Specific exergy (kJ/kg)
\dot{E}_x	Exergy (kW)
F	Faraday constant (C/mol)
F	Fuel
F_R	Removal factor
g	Gravity of earth (m/s ²)
G	Gibbs free energy (kJ)
G_b	Beam solar radiation (W/m ²)
h	Specific enthalpy (kJ/kg)
H	Enthalpy (kJ)
i	Interest rate
J	Density of flow (C/s)
J_0	Exchange current density (C/s)

APPENDIX A. ENERGY AND EXERGY EQUATIONS FOR SYSTEM A AND SYSTEM B

Table 1. Governing energy equations for all subsystems of system A and system B [27, 32, 40–44]

Subsystems	Governing energy equations
Parabolic trough collector	$\dot{m}_{in,oil} C_{p,oil} (T_{out,oil} - T_{in,oil}) = A_a F_R \left(S - \frac{A_r}{A_a} U_L (T_{in,oil} - T_0) \right)$ $\eta_{PTC} = \frac{F_R \eta_0 - U_L (T_{in,oil} - T_0) A_r}{G_b A_a}$
Biomass combustor	$\eta_{BC} \times (\dot{m}_{bio} LHV_{bio} + \dot{m}_{air} h_{air}) = \dot{m}_{in,w} (h_{out,w} - h_{in,w})$
Turbine	$\dot{W}_{turb} = \dot{m}_{in,w} (h_{in,w} - h_{out,w})$ $\eta_{is,turb} = \frac{\dot{W}_{turb}}{\dot{W}_{is,turb}}$
Pump	$\dot{W}_{turb} = \dot{m}_{in,w} (h_{in,w} - h_{out,w})$ $\eta_{is,turb} = \frac{\dot{W}_{turb}}{\dot{W}_{is,turb}}$
Double effect absorption chiller	$\dot{W}_{is,pump} = \dot{m}_{in,w} v_w (P_{out,w} - P_{in,w})$ $\eta_{is,pump} = \frac{\dot{W}_{is,pump}}{\dot{W}_{pump}}$
Heat exchanger	$\dot{E}_{heating} = \dot{m}_{in,w} (h_{out,w} - h_{in,w})$
Evaporator	$\dot{m}_{in,oil} C_{p,oil} (T_{in,oil} - T_{out,oil}) = \dot{m}_{in,w} (h_{out,w} - h_{in,w})$
Economizer	$\dot{m}_{in,oil} C_{p,oil} (T_{in,oil} - T_{out,oil}) = \dot{m}_{in,w} (h_{out,w} - h_{in,w})$
Multi effect desalination	$\dot{m}_{tot,pw} = \sum_i \dot{m}_{pw,eff,i}$ $\dot{m}_{in,exh} C_{p,exh} (T_{in,exh} - T_{out,exh}) = \dot{m}_{in} (h_{pw} - h_{sw})$
Liquefying natural gas	$\dot{W}_c = \dot{m}_{NG} T_{NG} \ln \left(\frac{P_{NG,out}}{P_{NG,in}} \right)$ $Y = \frac{\dot{m}_{LNG}}{\dot{m}_{NG}} = \frac{h_{NG,in} - h_{NG,out}}{h_{NG,in} - h_{LNG,sat}}$
Electrolyser	$\Delta H = \Delta G + T \Delta S$ $\dot{N}_{H_2,out} = \frac{J}{2F} = \dot{N}_{H_2O,reacted}$ $\dot{W}_{PEM} = J (V_0 + V_{act,a} + V_{act,c} + V_{ohm})$ $\theta[\lambda(x)] = \left[0.5139\lambda(x) - 0.326 \right] \exp \left[1268 \left(\frac{1}{303} - \frac{1}{T} \right) \right]$ $\lambda(x) = \frac{\lambda_a - \lambda_c}{D_L} x + \lambda_c, \quad R_{PEM} = \int_0^L \frac{dx}{\theta[\lambda(x)]}$ $J = J_{o,i} \left[\exp \left(\frac{\alpha ZF \lambda_{act,i}}{RT} \right) - \exp \left(\frac{(\alpha - 1) ZF \lambda_{act,i}}{RT} \right) \right], i = a, c$ $\lambda_{act,i} = \frac{RT}{F} \sinh^{-1} \left(\frac{J}{2J_{o,i}} \right), i = a, c$ $J_{o,i} = J_i^{ref} \exp \left(-\frac{E_{act,i}}{RT} \right), i = a, c$

APPENDIX B. EXERGOECONOMIC BALANCES FOR SUBSYSTEMS OF SYSTEM A AND SYSTEM B

Table 2. Governing exergy equations for all subsystems of system A and system B [27]

Subsystems	Exergy destruction rate	Exergy efficiency
Parabolic trough collector	$\dot{E}x_{D,PTC} = \dot{E}x_s - \dot{m}_{in,oil} (ex_{out,oil} - ex_{in,oil})$	$1 - \frac{\dot{E}x_{D,PTC}}{\dot{E}x_s}$
Biomass combustor	$\dot{E}x_{D,BC} = \dot{E}x_{bio} + \dot{m}_{air} ex_{air} - \dot{m}_{exh} ex_{exh} - \dot{m}_{in,w} (ex_{out,w} - ex_{in,w})$	$1 - \frac{\dot{E}x_{D,BC}}{\dot{E}x_{bio} + \dot{m}_{air} ex_{air}}$
Turbine	$\dot{E}x_{D,turb} = \dot{m}_{in,w} (ex_{in,w} - ex_{out,w}) - \dot{W}_{turb}$	$1 - \frac{\dot{E}x_{D,turb}}{\dot{m}_{in,w} (ex_{in,w} - ex_{out,w})}$
Pump	$\dot{E}x_{D,pump} = \dot{W}_{pump} - \dot{m}_{in,w} (ex_{out,w} - ex_{in,w})$	$1 - \frac{\dot{E}x_{D,pump}}{\dot{W}_{pump}}$
Double effect absorption chiller	$\dot{E}x_{D,DEAC} = \dot{m}_{in,w} (ex_{in,w} - ex_{out,w}) + \dot{E}x_{cooling} - \dot{E}x_{out,cond} - \dot{E}x_{out,abs}$	$1 - \frac{\dot{E}x_{D,DEAC}}{\dot{m}_{in,w} (ex_{in,w} - ex_{out,w})}$
Heat exchanger	$\dot{E}x_{D,HE} = \dot{m}_{in,w} (ex_{in,w} - ex_{out,w}) - \dot{E}x_{heating}$	$1 - \frac{\dot{E}x_{D,HE}}{\dot{m}_{in,w} (ex_{in,w} - ex_{out,w})}$
Evaporator	$\dot{E}x_{D,eva} = \dot{m}_{in,oil} (ex_{in,oil} - ex_{out,oil}) - \dot{m}_{in,w} (ex_{out,w} - ex_{in,w})$	$1 - \frac{\dot{E}x_{D,eva}}{\dot{m}_{in,oil} (ex_{in,oil} - ex_{out,oil})}$
Economizer	$\dot{E}x_{D,eco} = \dot{m}_{in,oil} (ex_{in,oil} - ex_{out,oil}) - \dot{m}_{in,w} (ex_{out,w} - ex_{in,w})$	$1 - \frac{\dot{E}x_{D,eco}}{\dot{m}_{in,oil} (ex_{in,oil} - ex_{out,oil})}$
Multi effect desalination	$\dot{E}x_{D,MED} = \dot{m}_{in,exh} (ex_{in,exh} - ex_{out,exh}) - (\dot{m}_{pw} ex_{pw} - \dot{m}_{sw} ex_{sw} - \dot{m}_{fw} ex_{fw}) - \dot{m}_b ex_b$	$1 - \frac{\dot{E}x_{D,MED}}{\dot{m}_{in,exh} (ex_{in,exh} - ex_{out,exh})}$
Liquefying natural gas	$\dot{E}x_{D,LNG} = \dot{W}_c - (\dot{m}_{LNG} ex_{LNG} - \dot{m}_{NG} ex_{NG})$	$1 - \frac{\dot{E}x_{D,LNG}}{\dot{W}_c}$
Electrolyser	$\dot{E}x_{D,PEM} = \dot{W}_{PEM} + \dot{E}_{PEM} - (\dot{m}_{H_2} ex_{H_2} + \dot{m}_{O_2} ex_{O_2})$	$1 - \frac{\dot{E}x_{D,PEM}}{\dot{W}_{PEM} + \dot{E}_{PEM}}$

APPENDIX B. EXERGOECONOMIC BALANCES FOR SUBSYSTEMS OF SYSTEM A AND SYSTEM B

Table 3. Exergoeconomic balances for all subsystems of system A and system B [14, 27, 45]

Subsystems	Exergoeconomic balance	Auxiliary relation	Purchase equipment cost, PEC (\$)
Parabolic trough collector	$\dot{C}_{in,oil} + \dot{Z}_{PTC} + \dot{C}_s = \dot{C}_{out,oil}$	$c_s = 0$	$PEC_{PTC} = 250 (A_a)$
Biomass combustor	$\dot{C}_{bio} + \dot{C}_{air} + \dot{C}_{in,w} + \dot{Z}_{BC} = \dot{C}_{out,w} + \dot{C}_{out,exh}$	$c_{out,exh} = 0$ $c_{air} = 0$ $c_{bio} = 0$	$PEC_{BC} = 1000 (\dot{Q}_{BC})$
Turbine	$\dot{C}_{in,w} + \dot{Z}_{turb} = \dot{C}_{out,w} + \dot{C}_{\dot{W}_{turb}}$	$c_{in,w} = c_{out,w}$	$PEC_{turb} = 3880.5 (\dot{W}_{turb})^{0.7} \left(1 + \left(\frac{0.05}{(1 - \eta_{is,turb})^3} \right) \right) \left(1 + 5 \left(\exp \left(\frac{T_m - 866}{10.42} \right) \right) \right)$
Pump	$\dot{C}_{in,w} + \dot{Z}_{pump} + \dot{C}_{\dot{W}_{pump}} = \dot{C}_{out,w}$	$c_{\dot{W}_{pump}} = c_{\dot{W}_{turb}}$	$PEC_{pump} = 3540 (\dot{W}_{pump})^{0.71}$
Double effect absorption chiller	$\dot{C}_{in,w} + \dot{Z}_{DEAC} = \dot{C}_{out,w} + \dot{C}_{cooling}$	$c_{in,w} = c_{out,w}$	$PEC_{DEAC} = 11595 (\dot{Q}_{cooling})^{0.73}$
Heat exchanger	$\dot{C}_{in,w} + \dot{Z}_{HE} = \dot{C}_{out,w} + \dot{C}_{heating}$	$c_{in,w} = c_{out,w}$	$PEC_{HE} = 130 \left(\frac{A_{HE}}{0.093} \right)^{0.78}$
Evaporator	$\dot{C}_{in,w} + \dot{C}_{in,oil} + \dot{Z}_{eva} = \dot{C}_{out,w} + \dot{C}_{out,oil}$	$c_{in,oil} = c_{out,oil}$	$PEC_{eva} = 130 \left(\frac{A_{eva}}{0.093} \right)^{0.78}$
Economizer	$\dot{C}_{in,w} + \dot{C}_{in,oil} + \dot{Z}_{eco} = \dot{C}_{out,w} + \dot{C}_{out,oil}$	$c_{in,oil} = c_{out,oil}$	$PEC_{eco} = 130 \left(\frac{A_{eco}}{0.093} \right)^{0.78}$
Multi effect desalination	$\dot{C}_{sw} + \dot{C}_{fw} + \dot{C}_{in,exh} + \dot{Z}_{MED} = \dot{C}_{out,exh} + \dot{C}_{pw} + \dot{C}_b$	$c_{sw} = 0$ $c_{in,exh} = c_{out,exh} = 0$ $c_b = 0$	$PEC_{MED} = 1542 (m_{pw})$
Liquefying natural gas	$\dot{C}_{NG} + \dot{C}_{\dot{W}_c} + \dot{Z}_{LNG} = \dot{C}_{LNG}$	$c_{\dot{W}_c} = c_{\dot{W}_{turb}}$	$PEC_{LNG} = 1400 (31536) (\dot{m}_{LNG})$
Electrolyser	$\dot{C}_{\dot{W}_{PEM}} + \dot{C}_{\dot{E}_{PEM}} + \dot{C}_{w,in} + \dot{Z}_{PEM} = \dot{C}_{H_2} + \dot{C}_{O_2}$	$c_{\dot{W}_{PEM}} = c_{\dot{W}_{turb}}$	$PEC_{PEM} = 1000 (\dot{W}_{PEM})$

J^{ref}	Pre-exponential factor
\dot{m}	Mass flow rate (kg/s)
m	Mass (kg)
n	Lifetime of the system
N	Annual operation hours
\dot{N}	Molar flow rate (mole/s)
P	Product
R	Universal gas constant
R_{PEM}	Overall ohmic resistance
s	Specific entropy (kJ/kg.K)
S	Heat absorbed by the receiver
System	System
T	Temperature (°C)
U_L	Coefficient of overall heat loss of collector ($W/m^2 \cdot K$)
V	Velocity (m/s)
V_0	Reversible potential
$V_{act,a}$	Activation potential of the anode
$V_{act,c}$	Activation potential of the cathode
V_{ohm}	Ohmic overpotential of the electrolyte
\dot{W}	Power (kW)
x	Molar fraction
x	Depth in the membrane (m)
y	Ratio of liquefied natural gas to natural gas
Z	Investment cost (\$)
Z	Height (m)
Z	Number of electrons involved per reaction
\dot{Z}	Investment cost rate (\$/s)

Greek Symbols

α	Symmetrical factor
η	Energy efficiency (%)
ε	Exergy efficiency (%)
η	Optical efficiency (%)
φ	Emission factor
λ	Water contents at the anode-membrane interface
λ_{act}	Activation overpotential of an electrode
λ_c	Water contents at the cathode-membrane interface
ν	Specific volume (m^3/kg)
δ	Maintenance factor
$\theta(x)$	Local ionic conductivity of the PEM

Abbreviation

CRF	Capital Recovery Factor
DEAC	Double Effect Absorption Chiller
EES	Engineering Equation Solver
ER	Emission Reduction
HHV	High Heating Value

HTG	High Temperature Generator
LHV	Low Heating Value
LiBr	Litume Bromide
LNG	Liquefying of Natural Gas
MED	Multi Effect Desalination
MSW	Municipal Solid Waste
PEC	Purchase Equipment Cost
PEM	Proton Exchange Membrane
PTC	Parabolic Trough solar Collector

Subscripts

0	Reference state
a	Anode
abs	Absorber of double effect absorption chiller
air	Air
b	brine
BC	Biomass Combustor
bio	biomass
c	Compressor
c	Cathode
cond	Condenser
D	Destruction
eff	Effect of multi effect desalination system
exh	Exhaust gas of biomass combustion
out	outlet
eco	Economizer
eva	Evaporator
fw	Feedwater
HE	Heat exchanger
i	Component/stream
in	Inlet
is	Isentropic
oil	Therminol VP-1 oil
pw	Fresh water
q	Heat
s	solar
ss	Strong solution of LiBr
sw	Sea water
tot	Total
Turb	Turbine
w	Work
w	Water
ws	Weak solution of LiBr

Superscripts

ch	Chemical
NG	Natural Gas

CI	Capital Investment
P	Product
FF	Fossil Fuel
OM	Operation and Maintenance
RN	Renewable energy
F	Fuel
ph	Physical

DATA AVAILABILITY STATEMENT

No new data were created in this study. The published publication includes all graphics collected or developed during the study.

CONFLICT OF INTEREST

The author declared no potential conflicts of interest with respect to the research, authorship, and/or publication of this article.

ETHICS

There are no ethical issues with the publication of this manuscript.

REFERENCES

- [1] Boyaghchi FA, Heidarnejad P. Thermoeconomic assessment and multi objective optimization of a solar micro CCHP based on Organic Rankine Cycle for domestic application. *Energy Convers Manag* 2015; 97: 224–234. doi: <https://doi.org/10.1016/j.enconman.2015.03.036>.
- [2] Jana K, De S. Sustainable polygeneration design and assessment through combined thermodynamic, economic and environmental analysis. *Energy* 2015; 91: 540–555. doi: <https://doi.org/10.1016/j.energy.2015.08.062>.
- [3] Caliskan H. Thermodynamic and environmental analyses of biomass, solar and electrical energy options based building heating applications. *Renew Sustainable Energy Rev* 2015; 43: 1016–1034. doi: <https://doi.org/10.1016/j.rser.2014.11.094>.
- [4] Noorpoor A, Heidarnejad P, Hashemian N, Ghasemi A. A thermodynamic model for exergetic performance and optimization of a solar and biomass-fuelled multigeneration system. *Energy Equip Syst* 2016; 4(2): 281–289. doi: <https://doi.org/10.22059/ees.2016.23044>.
- [5] Al Moussawi H, Fardoun F, Louahlia-Gualous H. Review of tri-generation technologies: Design evaluation, optimization, decision-making, and selection approach. *Energy Convers Manag* 2016; 120: 157–196. doi: <https://doi.org/10.1016/j.enconman.2016.04.085>.
- [6] Bellos E, Tzivanidis C. Parametric analysis and optimization of a solar driven trigeneration system based on ORC and absorption heat pump. *J Clean Prod* 2017; 161: 493–509. doi: <https://doi.org/10.1016/j.jclepro.2017.05.159>.
- [7] Khanmohammadi S, Heidarnejad P, Javani N, Ganjehsarabi H. Exergoeconomic analysis and multi objective optimization of a solar based integrated energy system for hydrogen production. *Int J Hydrog Energy* 2017; 42(33): 21443–21453. doi: <https://doi.org/10.1016/j.ijhydene.2017.02.105>.
- [8] Di Somma M, Yan B, Bianco N, Graditi G, Luh PB, Mongibello L, et al. Multi-objective design optimization of distributed energy systems through cost and exergy assessments. *Appl Energy* 2017; 204: 1299–1316. doi: <https://doi.org/10.1016/j.apenergy.2017.03.105>.
- [9] Calise F, Macaluso A, Piacentino A, Vanoli L. A novel hybrid polygeneration system supplying energy and desalinated water by renewable sources in Pantelleria Island. *Energy* 2017; 137: 1086–1106. doi: <https://doi.org/10.1016/j.energy.2017.03.165>.
- [10] Ganjehsarabi H, Asker M, Seyhan AK, editors. Energy and exergy analyses of a solar assisted combined power and cooling cycle. 2016 IEEE International Conference on Renewable Energy Research and Applications (ICRERA); 2016 20–23 Nov. 2016; Birmingham.
- [11] Sahoo U, Kumar R, Pant P, Chaudhary R. Development of an innovative polygeneration process in hybrid solar-biomass system for combined power, cooling and desalination. *Appl Therm Eng* 2017; 120: 560–567. doi: <https://doi.org/10.1016/j.applthermaleng.2017.04.034>.
- [12] Bellos E, Tzivanidis C. Multi-objective optimization of a solar driven trigeneration system. *Energy* 2018; 149: 47–62. doi: <https://doi.org/10.1016/j.energy.2018.02.054>.
- [13] Boyaghchi FA, Chavoshi M, Sabeti V. Multi-generation system incorporated with PEM electrolyzer and dual ORC based on biomass gasification waste heat recovery: Exergetic, economic and environmental impact optimizations. *Energy* 2018; 145: 38–51. doi: <https://doi.org/10.1016/j.energy.2017.12.118>.
- [14] Ghasemi A, Heidarnejad P, Noorpoor A. A novel solar-biomass based multi-generation energy system including water desalination and liquefaction of natural gas system: Thermodynamic and thermoeconomic optimization. *J Clean Prod* 2018; 196: 424–437. doi: <https://doi.org/10.1016/j.jclepro.2018.05.160>.

- [15] Khanmohammadi S, Atashkari K. Modeling and multi-objective optimization of a novel biomass feed polygeneration system integrated with multi effect desalination unit. *Therm Sci Eng Prog* 2018; 8: 269–283. doi: <https://doi.org/10.1016/j.tsep.2018.08.003>.
- [16] Yilmaz F. Thermodynamic performance evaluation of a novel solar energy based multigeneration system. *Appl Therm Eng* 2018; 143: 429–437. doi: <https://doi.org/10.1016/j.applthermaleng.2018.07.125>.
- [17] Wang Y, Wang X, Yu H, Huang Y, Dong H, Qi C, et al. Optimal Design of Integrated Energy System Considering Economics, Autonomy and Carbon Emissions. *J Clean Prod* 2019. doi: <https://doi.org/10.1016/j.jclepro.2019.03.025>.
- [18] Nalbant Y, Colpan CO, Devrim Y. Energy and exergy performance assessments of a high temperature-proton exchange membrane fuel cell based integrated cogeneration system. *Int J Hydrog Energy* 2019. doi: <https://doi.org/10.1016/j.ijhydene.2019.01.252>.
- [19] Ganjehsarabi H. Mixed refrigerant as working fluid in Organic Rankine Cycle for hydrogen production driven by geothermal energy. *Int J Hydrog Energy* 2019; 44(34): 18703–18711. doi: <https://doi.org/10.1016/j.ijhydene.2018.11.231>.
- [20] Mateus T, Oliveira AC. Energy and economic analysis of an integrated solar absorption cooling and heating system in different building types and climates. *Appl Energy* 2009; 86(6): 949–957. doi: <https://doi.org/10.1016/j.apenergy.2008.09.005>.
- [21] Jiang-Jiang W, Chun-Fa Z, You-Yin J. Multi-criteria analysis of combined cooling, heating and power systems in different climate zones in China. *Appl Energy* 2010; 87(4): 1247–1259. doi: <https://doi.org/10.1016/j.apenergy.2009.06.027>.
- [22] Sigarchian SG, Malmquist A, Martin V. Design Optimization of a Small-Scale Polygeneration Energy System in Different Climate Zones in Iran. *Energies* 2018; 11(5): 1–19. doi: <https://doi.org/10.3390/en11051115>.
- [23] Heidarnejad P, Noorpoor A, Dincer I. Chapter 2.19 - Thermodynamic and Thermo-economic Comparisons of Two Trigeration Systems. In: Dincer I, Colpan CO, Kizilkan O, editors. *Exergetic, Energetic and Environmental Dimensions*: Academic Press; 2018. p. 551–567.
- [24] Doseva N, Chakyrova D. Energy and Exergy Analysis of Cogeneration System with Biogas Engines. *Journal of Thermal Engineering* 2015; 1(3): 391–401. doi: 10.18186/jte.75021.
- [25] Chakyrova D, Doseva N. Thermo-economic Analysis of Biogas Engines Powered Cogeneration System. *Journal of Thermal Engineering* 2019; 5(2): 93–107. doi: 10.18186/thermal.532210.
- [26] Klein SA. Engineering Equation Solver (EES). from <https://fchart.com/ees/>; 2013.
- [27] Frangopoulos CA. *Exergy, Energy System Analysis and Optimization-Volume I: Exergy and Thermodynamic Analysis*. UK: EOLSS Publications, 2009.
- [28] NASA Surface meteorology and Solar Energy. 2013. Available from: <https://eosweb.larc.nasa.gov/cgi-bin/sse/daily.cgi/>.
- [29] Bejan A, Tsatsaronis G, Moran M. *Thermal design and optimization*. Canada: John Wiley & Sons Inc., 1996.
- [30] Frangopoulos CA. *Exergy, Energy System Analysis and Optimization-Volume II: Thermo-economic Analysis, Modeling, Simulation and Optimization in Energy Systems*. UK: EOLSS Publications, 2009.
- [31] Hugot E. *Handbook of cane sugar engineering*. USA: Elsevier, 2014.
- [32] Tchobanoglous G, Theisen H, Vigil S. *Integrated solid waste management: engineering principles and management issues*. 2nd ed. USA: McGraw Hill, 1993.
- [33] *Compilation of air pollutant emission factors 1: Stationary Point and Area Sources Chapter 3: Stationary Internal Combustion Sources, AP-42*. New York: EPA, 1979.
- [34] EPA. *Compilation of air pollutant emission factors*. New York: Environmental Protection Agency, 1979.
- [35] AP-42, *Compilation of air pollutant emission factors, Volume 1: Stationary Point and Area Sources Chapter 2: Solid Waste Disposal* New York: EPA, 1979.
- [36] *Emission Factor for Greenhouse Gas Inventories*. 2018. Available from: https://epa.gov/sites/production/files/2018-03/documents/emission-factors_mar_2018_0.pdf.
- [37] Bernt J. *Good Practice Guidance and Uncertainty Management in National Greenhouse Gas Inventories: Emissions from Waste Incineration*. Montreal: IPCC, 2000.
- [38] Ioroi T, Yasuda K, Siroma Z, Fujiwara N, Miyazaki Y. Thin film electrocatalyst layer for unitized regenerative polymer electrolyte fuel cells. *Journal of Power sources* 2002; 112(2): 583–587. doi: 10.1016/S0959-6526(01)0583-5.
- [39] Al-Sulaiman FA. Exergy analysis of parabolic trough solar collectors integrated with combined steam and organic Rankine cycles. *Energy Convers Manag* 2014; 77: 441–449. doi: 10.1016/j.enconman.2014.05.011.
- [40] Cengel AY, Boles MA. *Thermodynamics: An engineering approach*. New York: McGraw Hill, 2008.
- [41] Kalogirou S. *solar energy engineering: processes and systems*. UK: Elsevier, 2009.
- [42] Dincer I. *Refrigeration systems and applications*. UK: John Wiley & Sons, 2017.

-
- [43] Ni M, Leung MK, Leung DY. Energy and exergy analysis of hydrogen production by a proton exchange membrane (PEM) electrolyzer plant. *Energy Convers Manag* 2008; 49(10): 2748–2756. doi: <https://doi.org/10.1016/j.enconman.2008.03.018>.
- [44] Gurau V, Barbir F, Liu H. An analytical solution of a half-cell Model for PEM fuel cells. *J Electrochem Soc* 2000; 147(7): 2468–2477. doi: <https://doi.org/10.1149/1.1393555>.
- [45] Kotas TJ. *The exergy method of thermal plant analysis*. Reprint ed. Malabar, Fla.: Krieger Pub., 1995.